Dietary and biliary phosphatidylcholine activates PKCζ in rat intestine[S]

Shahzad Siddiqi* and Charles M. Mansbach II[1,*,†]

Division of Gastroenterology,* The University of Tennessee Health Science Center, Memphis, TN; and Veterans Affairs Medical Center,[†] Memphis, TN

Abstract **Chylomicron output by the intestine is proportional to intestinal phosphatidylcholine (PC) delivery. Using five different variations of PC delivery to the intestine, we found that lyso-phosphatidylcholine (lyso-PC), the absorbed form of PC, concentrations in the cytosol (0 to 0.45 nM) were proportional to the input rate. The activity of protein kinase C (PKC)ζ, which controls prechylomicron output rate by the endoplasmic reticulum (ER), correlated with the lyso-PC concentration suggesting that it may be a PKCζ activator. Using recombinant PKCζ, the K_m for lyso-PC activation was 1.49 nM and the V_{max} 1.12 nM, more than the maximal lyso-PC concentration in cytosol, 0.45 nM. Among the phospholipids and their lyso derivatives, lyso-PC was the most potent activator of PKCζ and the only one whose cytosolic concentration suggested that it could be a physiological activator because other phospholipid concentrations were negligible. PKCζ was on the surface of the dietary fatty acid transport vesicle, the caveolin-1-containing endocytic vesicle. Once activated, PKCζ, eluted off the vesicle. A conformational change in PKCζ on activation was suggested by limited proteolysis. We conclude that PKCζ on activation changes its conformation resulting in elution from its vesicle. The downstream effect of dietary PC is to activate PKCζ, resulting in greater chylomicron output by the ER.—**Siddiqi, S., and C. M. Mansbach II. **Dietary and biliary phosphatidylcholine activates PKCζ in rat intestine. *J. Lipid Res.* 2015.** 56: **859–870.**

Supplementary key words protein kinase C zeta • lyso-phosphatidylcholine • caveolin-1-containing endocytic vesicle • chylomicrons

Because obesity and its attendant health issues are a major health problem not only in the United States but also throughout the developed world, potential mechanisms for its mitigation are of increasing importance. One possibility is to block absorbed lipid export from the intestine. The intestine takes dietary FAs and *sn*-2-monoacylglcyerols (MAGs), the lipolytic products of dietary fat, and converts them to triacylglycerols (TAGs) at the level of the endoplasmic reticulum (ER). These TAGs are incorporated into the intestinal-specific TAG-rich lipoprotein prechylomicron for export from the lumen of the ER to the Golgi. This export step is performed by a specialized transport vesicle, the prechylomicron transport vesicle (PCTV) (1). The exit of prechylomicrons from the ER in PCTV is the rate-limiting step in the transit of dietary lipid across the enterocyte (2, 3). Inhibiting PCTV formation or its fission step from the ER could potentially block absorbed lipid at the level of the enterocyte. The molecular events associated with PCTV formation and their targeting to the Golgi have been recently elucidated (1, 4, 5). This knowledge could lead to specific targets for inhibition of this process.

Recent data suggest that the ER export step for prechylomicrons is potentially regulatable by control of the amount of liver fatty acid binding protein (FABP) 1 able to bind to the ER. We have shown that FABP1 can organize a set of four proteins that can select prechylomicrons as cargo and bud PCTV from the ER membrane (4, 6). We have further found that the binding of FABP1 to the ER to initiate budding is, in turn, controlled by its release from a four-membered cytosolic protein complex present in intestinal cytosol. In the absence of release from the complex, FABP1 cannot bind to the ER (7). The disruption of the complex is controlled by the phosphorylation of Secretion Associated, Ras Related GTPase 1B (Sar1b). We have identified the kinase performing this function as protein kinase C (PKC)ζ (8). On Sar1b phosphorylation, the heteroquatromer is completely disrupted, releasing FABP1 (7).

PKCζ is a member of a family of protein kinases, the atypical protein kinases, which do not require either diacylglycerol (DAG) or Ca^{2+} for their activation. Assays for

This work was supported by a Veterans Administration Merit Award (C.M.M.).

Manuscript received 12 November 2014 and in revised form 23 February 2015.

Published, JLR Papers in Press, February 24, 2015
DOI 10.1194/jlr.M056051

Abbreviations: CEV, caveolin-1-containing endocytic vesicle; DAG, diacylglycerol; DRM, detergent resistant membrane; ER, endoplasmic reticulum; FABP, fatty acid binding protein; lyso-PC, lysophosphatidylcholine; MAG, monoacylglycerol; PC, phosphatidylcholine; PCTV, prechylomicron transport vesicle; PKC, protein kinase C; PS, phosphatidylserine; rPKCζ, recombinant PKCζ; Sar1b, Secretion Associated, Ras Related GTPase 1B; TAG, triacylglycerol; TC, taurocholate; TO, triolein; VAMP, vesicle associated membrane protein.

[1]To whom correspondence should be addressed.
e-mail: cmansbach@uthsc.edu

[S] The online version of this article (available at http://www.jlr.org) contains supplementary data in the form of one figure.

PKCζ typically contain phosphatidylserine (PS) as activator. Because the amount of PS required for PKCζ activation is greater than that present in intestinal cytosol, we hypothesized that a different activator was operative. The hypothesis tested in this report is that lyso-phosphatidylcholine (lyso-PC) is the physiological activator of PKCζ in the intestine. We focused on lyso-PC because it has long been known that the amount of phosphatidylcholine (PC) delivered to the intestine correlates with chylomicron output into the lymph (9). Prior to its absorption, PC must be hydrolyzed to *sn*-1 lyso-PC by pancreatic phospholipase A_2. In accord with this hypothesis, bile diversion or *mdr2* knockout mice, which are not able to deliver PC to the bile, are associated with the lowest chylomicron output by the intestine (10, 11); whereas fat feeding, which increases biliary PC output (12), and PC supplementation both increase chylomicron output (13) as compared with chow-fed controls. These data were obtained using the same intraduodenal TAG input rates. In the past, the correlation between chylomicron output and PC delivery to the intestine has been thought to be due to the availability of PC for chylomicron surface formation. We provide evidence of an alternative mechanism in this report.

MATERIALS AND METHODS

Materials

[^{3}H]oleic acid (9.2 Ci/mM) and [^{3}H]PC (32.7 Ci/mM) were obtained from Perkin Elmer Life Sciences (Waltham, MA). Lyso-PC, lyso-phosphatidylserine (lyso-PS), lyso-phosphatidylinositol (lyso-PI), and lyso-phosphatidylethanolamine (lyso-PE) were purchased from Avanti Polar Lipids (Alabaster, AL). Iodixanol (OptiPrep) was purchased from Sigma (Sigma Chemical Co., St. Louis, MO). ECL reagents were procured from GE Healthcare (Fairfield, CT). Protease inhibitor cocktail tablets were obtained from Roche Applied Sciences (Indianapolis, IN). Immunoblot reagents were purchased from Bio-Rad (Hercules, CA). Other biochemicals used were of analytical grade from Sigma (Sigma Chemical Co.) or local companies. Male Sprague Dawley rats, 150–250 g were purchased from Harlan Laboratories (Indianapolis, IN). Rat chow containing 23% fat (w/w, composition 21% milk fat, 2% soybean oil) in pellet form was obtained from Harlan Laboratories.

Antibodies

Rabbit polyclonal antibodies against CD36, caveolin-1, PKCζ, and goat polyclonal antibodies against intestinal alkaline phosphatase were all purchased from Santa Cruz Biotechnology (Santa Cruz, CA). PKCζ substrate-biotinylated was obtained from Santa Cruz Biotechnology. Biotinylated Anti-Rabbit IgG (H+L) antibody was purchased from KPL (Gaithersburg, MD). Streptavidin, HRP conjugate was procured from EMD Millipore Co. (Billerica, MA). Anti-rabbit IgG conjugated with agarose beads was purchased from Sigma Chemical Co. Goat anti-rabbit IgG and goat anti-mouse IgG conjugated with HRP were also procured from Sigma. PKCζ was purchased from Enzo Life Sciences Inc. (Farmingdale, NY).

Animal preparation

Intraduodenal infusion of male Sprague-Dawley rats (200–300 g) was performed as described previously (14). In brief, five groups (A to E) of rats participated in the experiments. All the animals were maintained on a chow diet (4% fat, w/w) except group D, which was placed on a high-fat diet (23% fat, w/w) for 2 weeks prior to the experiment. All rats received duodenal cannulas (PE 50) 1 day prior to the experiments and were infused intraduodenally with 0.15 M NaCl, 0.3 M KC1, and 5% glucose at 3 ml/h overnight. Group A rats had their bile duct cannulated (PE 10) in addition to their duodenal cannulas. The next day, the infusion for groups A and B was changed to 0.15 M NaCl. The infusions for groups C and D were changed to 30 mM triolein (TO), 10 mM taurocholate (TC), 0.15 M NaCl, and 10 mM Tris-HC1 (pH 7.4). Group E was given the same TO infusion supplemented with 2 mM PC. All infusions were at 4.5 ml/h for 4 h and were supplemented with [^{3}H]oleate TO (10×10^6 dpm/ml). A summary of the models used is presented in **Table 1**. After the 4 h infusion was completed, all of the groups were treated identically. The rats were given an overdose of pentobarbital, and the proximal one-half of the small intestine was removed, flushed with ice-cold 0.15 M NaC1, and placed in iced saline.

Isolation of cytosol

Enterocytes from the proximal half of rat small intestine were isolated as described previously (1). In brief, enterocytes were isolated from intestinal villi (15) homogenized using a Parr bomb, and the cytosol was isolated by centrifugation. The isolated cytosol was dialyzed against buffer A [0.25 M sucrose, 30 mM HEPES (pH 7.2), 30 mM KCl, 5 mM $MgCl_2$, 5 mM $CaCl_2$, 2 mM DTT] overnight at 4°C. This cytosol was concentrated on a Centricon filter (Amicon, Beverly, MA) with a 10 kDa cutoff to 20 mg of protein/ml.

Isolation of caveolin-1-containing endocytic vesicles from cytosol

Caveolin-1-containing endocytic vesicles (CEVs) were isolated as described previously (16). In brief, cytosol (1 mg protein) was treated with 1% Triton X-100. The treated cytosol was placed at the bottom of an OptiPrep step gradient (0 to 35%), and the gradient was centrifuged for 20 h at 4°C. The gradient was resolved by collecting nine 1 ml fractions using a pipette starting at the top of the gradient. One hundred microliters from each fraction was collected for radioactivity determination. The proteins in each fraction were precipitated with TCA, washed twice with cold acetone, and suspended in Laemmli's buffer. The proteins were separated by SDS-PAGE and identified by immunoblot using specific antibodies as indicated.

Distribution of absorbed [^{3}H]PC in CEV after corn oil gavage

Nonfasting rats were anesthetized and gavaged with 0.5 ml corn oil containing [^{3}H]PC (12×10^6 dpm). Thirty minutes later, the rats were euthanized and the proximal half intestines removed. Enterocytes were isolated, and cytosol was obtained as described above. CEVs were isolated by OptiPrep gradient. Ninety-two percent of the cytosolic radioactivity was in lyso-PC.

Extraction of phospholipids from cytosol

Phospholipids were extracted from cytosol by chloroform-methanol extraction. Two milliliters of $CHCl_3$/methanol (2:1) was added to 100 μl of cytosol and agitated vigorously. The extracts were centrifuged at 9000 *g* for 5 min at 4°C. Five hundred microliters of 0.9% NaCl was added to the bottom layer, mixed vigorously, and recentrifuged as described above. The chloroform layer was collected and evaporated under nitrogen for quantitation.

TABLE 1. Infusion conditions for rat models of increasing PC delivery to the intestine

Rat Model	Pretreatment	Infusion Composition	Expected PC Delivery
A	Bile duct diversion	Saline	0
B	Chow fed	Saline	+
C	Chow fed	TC + TO	++
D	7 day fat fed[a]	TC + TO	+++
E	Chow fed	TC + TO + PC	++++

[a]Twenty-three percent fat (w/w).

Quantitation of lyso-PC

Phospholipids in cytosol were first quantified as described by McHowat and Corr (17). In brief, samples were injected onto an Ascentis Si 5-μm HPLC (25 cm × 4.6 mm) column (Supelco Analytical, Sigma Chemical Co.) and eluted with a mobile phase of hexane-isopropyl alcohol-water (45:50:5) at a flow rate of 1.0 ml/min. Absorbance was measured at 203 nm. Samples were also quantitated radiometrically using [^{14}C]acidic anhydride (10 mCi/mM; ARC, St. Louis, MO). Samples were treated as suggested by Wientzek et al. (18). In brief, the lipids from cytosol were extracted as above, and the lyso-PC was isolated from a silicic acid column using chloroform-methanol (1:9) after other lipids had been removed by passing progressively more methanol in chloroform over the column. The lyso-PC was treated with [^{14}C]acidic anhydride (20,000 dpm), and the acetylated lyso-PC was separated by TLC. Its radioactivity was determined and compared with known quantities of lyso-PC treated similarly.

PKCζ activity assays

PKCζ activity in cytosol was quantified using a modified method described by Calbiochem (EMD Millipore Co.). In brief, to bind biotinylated anti-rabbit antibody to agarose beads, we incubated 10 μl biotinylated anti-rabbit antibody with 100 μl of anti-rabbit agarose beads for 3 h at 4°C. After incubation, the beads were washed three times with PBS. Recombinant PKCζ (rPKCζ) in 100 μl of buffer B (250 mM Tris-HCl, pH 7.0, 30 mM $MgCl_2$, 5 mM EDTA, 10 mM EGTA, 50 mM β-mercaptoethanol), 15 μl of 1 mM ATP, 15 μl of 0 to 40 nM PS or 0 to 10 nM of lyso-PC, and 65 μl water were incubated with 2 μl of biotinylated PKCζ substrate for 5 min at 37°C. The reaction was stopped with 500 μl of cold PBS. The reaction mixture was added to anti-rabbit agarose beads as described above for 3 h at 4°C. After incubation, the beads were washed with cold PBS three times and suspended in 400 μl of PBS. Five microliters of HRP-conjugated streptavidin was added to the suspension and incubated for 2 h at 4°C, washed three times with cold PBS, followed by the addition of 100 μl of substrate (5 mg *o*-phenylenediamine in 5 ml of H_2O_2), and incubated for 5 min at room temperature. The reaction was stopped with 100 μl of 20% H_3PO_4, and 2 ml of PBS was added. The supernatant was obtained by centrifugation and read at 492 nm.

Immunodepletion of PKCζ

Immunodepletion was performed by immunoadsorption (1). Briefly, cytosol (1 mg) was incubated with 20 μl of anti-PKCζ rabbit polyclonal antibodies at 4°C for 4 h, and then anti-rabbit IgG conjugated with agarose beads was added. The mixture was slowly agitated for 4 h at 4°C. The antibody-protein complexes were removed by centrifugation. Successful depletion of PKCζ from cytosol was obtained by three rounds of immunodepletion and confirmed by immunoblotting.

Conditions for binding or elution of PKCζ from CEV

Fifty micrograms of CEV was incubated with 6 nM of lyso-PC in 100 μl of buffer C (250 mM Tris-HCl, pH 7.0, 30 mM $MgCl_2$, 5 mM EDTA, 10 mM EGTA, 50 mM β-mercaptoethanol), 15 μl of 1 mM ATP, and 65 μl water for 30 min at 4°C. The reaction was stopped by adding 500 μl of cold PBS. CEVs were reisolated by OptiPrep step gradient as described above. Repopulation of CEVs by activated PKCζ was performed by the incubation of 500 μg PKCζ depleted cytosol with 1 nM of activated rPKCζ (incubated with 6 nM lyso-PC) in a total volume of 500 μl buffer D (0.25 M sucrose, 30 mM HEPES, pH 7.2, 30 mM KCl, 5 mM $MgCl_2$, 5 mM $CaCl_2$, 2 mM DTT) with an ATP regenerating system (1 mM ATP, 5 mM phosphocreatine, and 5 U creatine phosphokinase) for 30 min at 4°C. CEVs were reisolated using an OptiPrep gradient. The proteins from each fraction were separated by SDS-PAGE and identified by immunoblot using PKCζ antibodies.

Proteolysis method

Native and lyso-PC-activated PKCζ were subjected to tryptic digestion. Digestions were carried out at 37°C for 0, 2, 4, 8 min by using an enzyme-protein mass ratio of 1:200. Reactions were terminated by adding Laemmle's buffer and boiled for 5 min. The proteolytic digestion products were resolved on SDS-PAGE followed by silver staining.

Immunoprecipitation of proteins

Cytosol (1 mg) was incubated with 20 μl of specific rabbit antibodies at 4°C for 4 h, anti-rabbit IgG conjugated with agarose beads was added, and the mixture was stirred slowly at 4°C overnight. The beads were removed by centrifugation, washed 10 times with cold PBS, and resuspended in Laemmli's buffer for immunoblot analysis.

SDS-PAGE and immunoblot

Proteins were separated by SDS-PAGE and then transblotted to nitrocellulose membranes (Bio-Rad). After incubation with specific primary antibodies and peroxidase-conjugated secondary antibodies, labeled proteins were detected using ECL (Amersham Biosciences) and Biomax film (Eastman Kodak, Rochester, NY).

Measurement of TAG and phospholipid radioactivity

TAG radioactivity was determined by liquid scintillation as described (16). Phospholipids were similarly measured.

RESULTS

[^{3}H]oleate is absorbed via CEV under varying PC infusion conditions

Because we planned to greatly vary the PC input rate into the intestine, we first wished to be certain that the variation either in the delivery of PC to the intestinal lumen in our models or the flux of lyso-PC into the intestinal

cytosol did not affect the mechanism of FA absorption. Absorbed FA enters the cytosol on a CEV and appears in the detergent resistant membrane (DRM) fraction of an OptiPrep gradient (16). Despite the wide variation in the PC intake (0–9 μmol/h), the FA tracer, [^{3}H]oleate, remained in the DRM in cytosol, consistent with our prior observations (**Fig. 1A–**E, Table 1). Under all experimental conditions, caveolin-1, CD36, and PKCζ tracked with the [^{3}H]oleate in the DRM. We have previously shown that the detergent soluble fraction in the OptiPrep gradient contains the expected clathrin (16).

These data suggest the possibility that lyso-PC would also be associated with CEV. To test this, rats were gavaged with corn oil supplemented with PC and [^{3}H]PC. After 30 min, the intestine was harvested, and the cytosolic fraction was obtained. Ninety-two percent of the total cytosolic dpm were in lyso-PC. To determine the percentage of the lyso-PC dpm in CEV, we placed the cytosol on an OptiPrep gradient. We found that the majority (69%) of the lyso-PC in cytosol was in the DRM fraction as suggested by its distribution in the OptiPrep gradient. These data are consistent with the lyso-PC being in the CEV (**Fig. 2**).

Lyso-PC concentrations in cytosol vary with PC delivery conditions

It would be predicted that altering the intake of lyso-PC from the intestinal lumen would be reflected in the concentration of lyso-PC in the cytosol. To see if this were so, we measured the lyso-PC concentration in intestinal cytosol in each of our models by HPLC at 203 nm (**Fig. 3A**). To determine whether the signal at 203 nm was due solely to lyso-PC, we performed LC/MS/MS on a sample (supplementary Fig. 1). The spectrum obtained confirmed that the signal at 203 nm was lyso-PC. Because absorption at 203 nm may in part be due to artifacts, we also performed a radiometric assay on each sample. Lyso-PC was isolated by silicic acid column chromatography and acetylated using [^{14}C]acetic anhydride. The acetylated lyso-PC was separated by TLC, and its radioactivity was determined. Similarly treated lyso-PC standards were used for

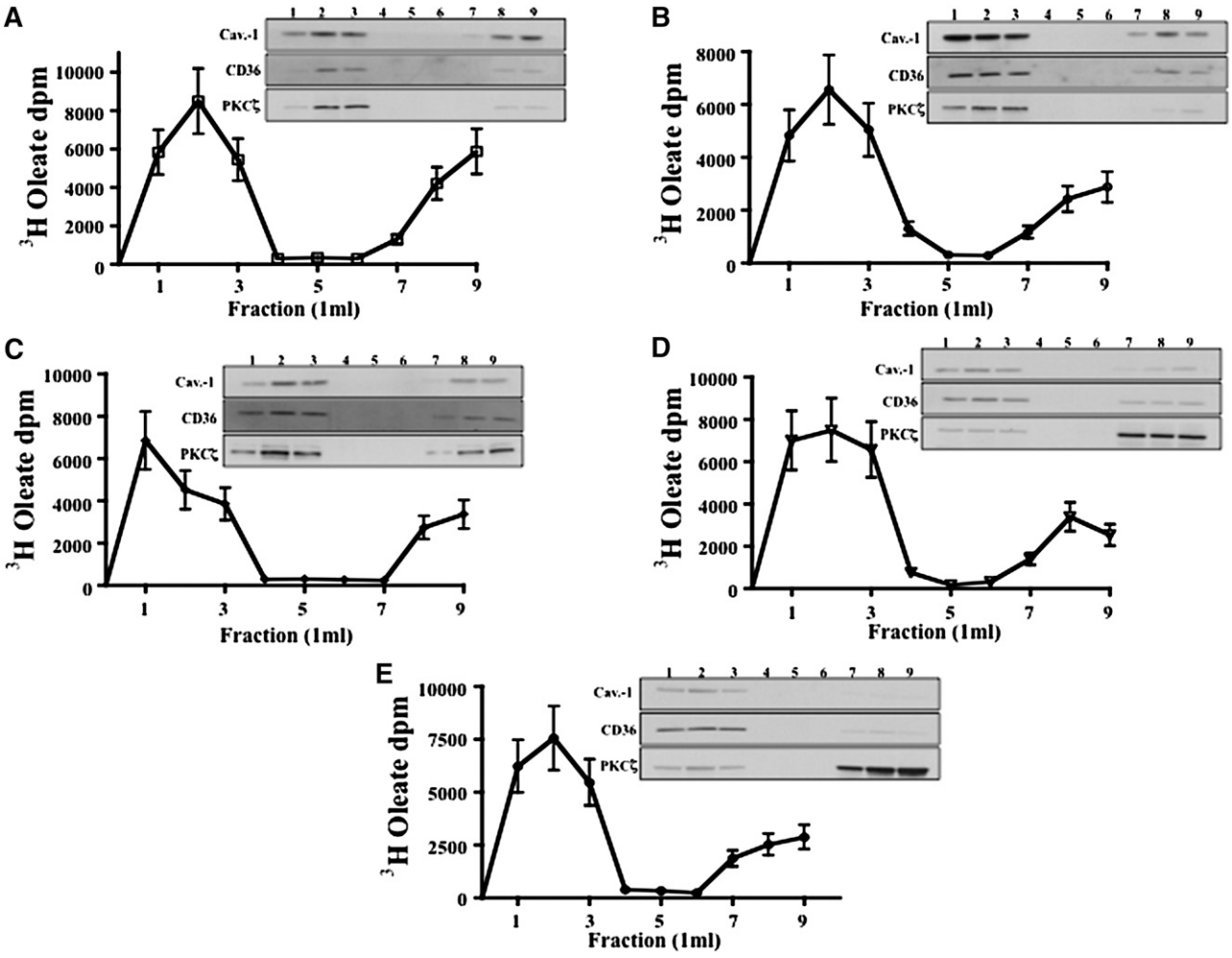

Fig. 1. The distribution of cytosolic [^{3}H]oleate in an OptiPrep gradient from rat intestinal cytosol infused with varying amounts of PC. The models used were as follows: bile diversion (A), saline infused (B), TO infused (C), and 2 weeks high-fat diet (23% w:w) (D), PC infused, 9 μmol/h (E). At the conclusion of the 4 h, infusion (Materials and Methods), the proximal half intestine was harvested. Cytosol was obtained and placed on top of an OptiPrep gradient. The gradient was resolved, fractions were collected from the top of the gradient, and radioactivity was determined. Immunoblots for caveolin-1, CD36, and PKCζ are shown above the graphs for each fraction (Materials and Methods).

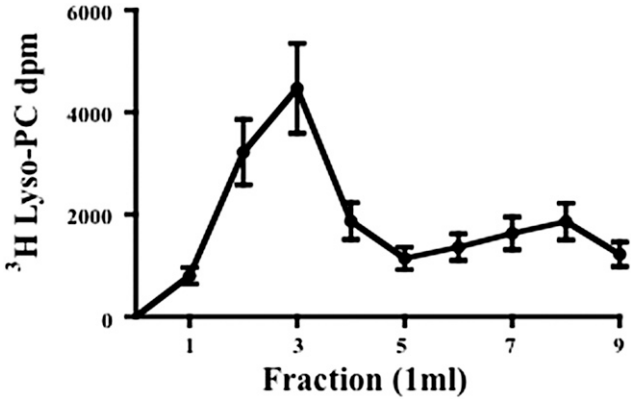

Fig. 2. The distribution of [^{3}H]lyso-PC in an OptiPrep gradient from intestinal cytosol. Rats were gavaged with 0.5 ml corn oil containing [^{3}H]PC. Thirty minutes later, the proximal half of the intestine was removed, and cytosol was prepared (Materials and Methods). The cytosol was placed on an OptiPrep gradient, the gradient was resolved, and fraction was collected from the top of the gradient. Radioactivity was determined in each fraction (ordinate). Ninety-two percent of the total radioactivity in cytosol was in lyso-PC.

quantitation. The results of this alternative assay (Fig. 3B) agreed closely (5–20% greater) with the quantitation using 203 nm (Fig. 3A).

As expected, the lyso-PC concentration in the cytosol varied with the input rate (Fig. 3A, B). Because most of the PC delivered to the intestine comes from bile (19), bile diversion should result in a reduction in cytosolic lyso-PC over bile intact rats. In agreement with this expectation, only negligible amounts of lyso-PC were found in this model (Fig. 3A, B). By contrast, the maximal amount of lyso-PC was found when PC was included in the intraduodenal TO infusion, 0.46 nM (Fig. 3A, B). We also analyzed the cytosol for PC, PS, phosphatidylethanolamine, and phosphatidylinositol, but only negligible amounts were found (data not shown). Similarly, the lyso derivatives of each phospholipid except PC were present in very small amounts (data not shown).

PKCζ activity varies with cytosolic lyso-PC concentration

Our major interest was whether the changes in cytosolic lyso-PC were associated with alterations in PKCζ activity. To determine PKCζ activity in our models, we first wished to know the range of cytosolic protein concentrations associated with rates of PKCζ activity proportional to the PKCζ added (**Fig. 4A**). All subsequent PKCζ activity measurements used protein concentrations of 40 μg or less. As shown in Fig. 4B, PKCζ activity closely tracked the concentration of lyso-PC in the cytosol (Fig. 3). The lowest activity was found in the bile diversion model, and the highest activity was found when PC was included in the intraduodenal TO infusion model with a 34-fold difference between them. These changes in enzyme activity were not due to alterations in the quantity of PKCζ as judged by immunoblot (Fig. 4C).

Lyso-PC activates PKCζ

The correlation of lyso-PC concentrations in the cytosol with PKCζ activity suggested that lyso-PC might be an activator of PKCζ. To directly test this, we incubated rPKCζ with ATP and increasing amounts of lyso-PC. The results (**Fig. 5A**) show a robust response in PKCζ activity on the addition of lyso-PC suggesting that lyso-PC is a potent PKCζ activator. Importantly, the calculated K_m of 1.49 nM for lyso-PC activation is above the values found for lyso-PC concentrations in the cytosol in our models. This implies that changes in lyso-PC concentrations in our models would have a direct effect on PKCζ activity confirming the data in Fig. 4. Because PS is a well-known activator of PKCζ, we also tested PKCζ activity with increasing amounts of PS.

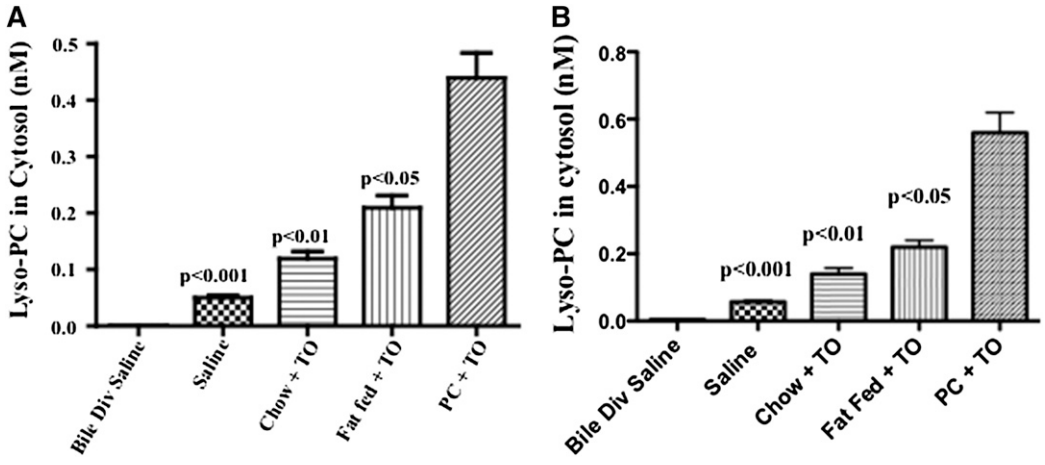

Fig. 3. The concentration of lyso-PC in cytosol under varying input rates of PC into the intestine. Intestinal cytosol was prepared from the proximal half of the intestine using experimental conditions as in Fig. 1, and phospholipids were extracted (Materials and Methods). A: Lyso-PC was quantitated by HPLC at 203 nm. B: Lyso-PC was separated using a silicic acid column and quantitated radiometrically after acetylation using [^{14}C]acidic anhydride (Materials and Methods). The *P* values above the bars test the differences between the means of the PC-infused rats with the other groups. However, each group was significantly different ($P < 0.05$) from the next group with more lyso-PC in the cytoplasm.

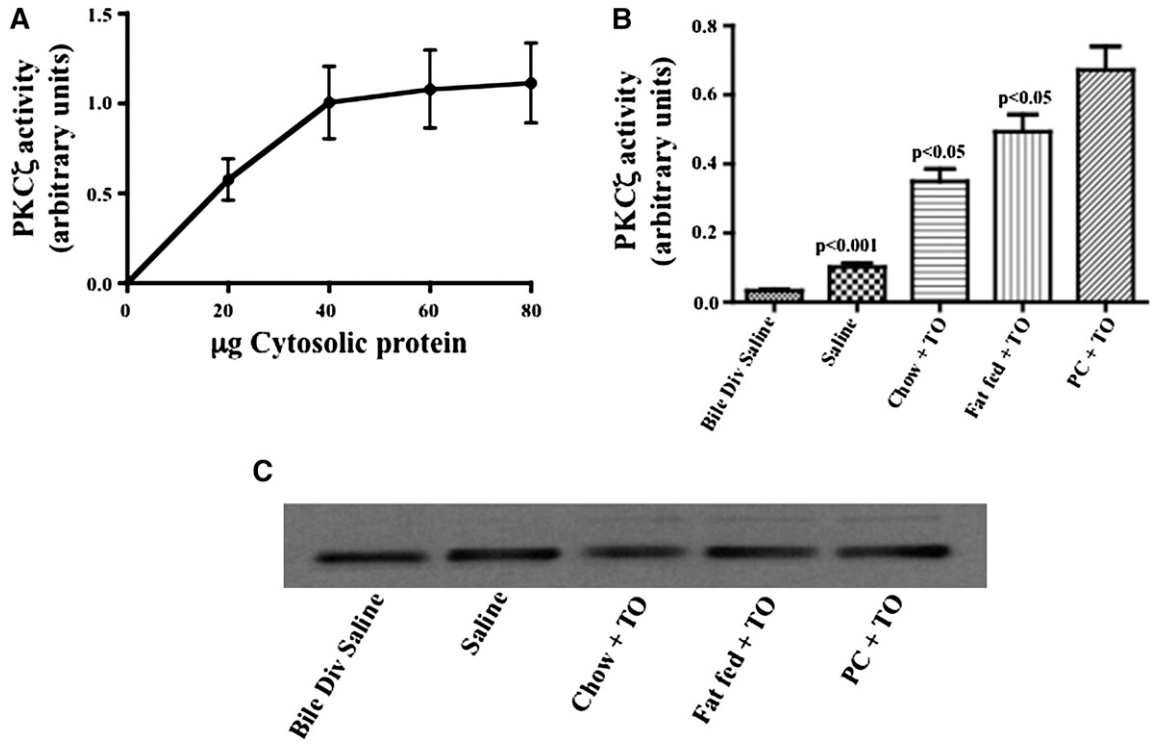

Fig. 4. PKCζ activity under varying rates of PC delivery to the intestine. A: PKCζ activity was measured on the addition of the indicated amounts of cytosolic protein. The data are expressed in arbitrary units on the ordinate. B: PKCζ activity under varying physiological conditions. Intestinal cytosol was prepared from the proximal half of the intestine using the experimental conditions as outlined in Fig. 1. PKCζ activity was measured in each model, and the results in arbitrary units are displayed on the ordinate. C: Immunoblot for cytosolic PKCζ in each model (Fig. 1A–E). Thirty micrograms of cytosolic protein was loaded in each lane. *P* values are indicated above the bars.

As expected, PS also activated PKCζ (Fig. 5B) but with a reduced potency as compared with lyso-PC with a K_m of 41 nM, 28-fold greater than lyso-PC. Importantly, the concentration of PS in our models was so low that it would not be expected to be an effective activator of PKCζ (data not shown).

Because lyso-PC is a detergent, we wondered if this property activated PKCζ or if there were a more specific interaction between the two. To test this, we used both SDS and Triton X-100 (1%), a concentration similar to what was used to isolate CEV. Both detergents were ineffective as activators (0.03% and 0.09% the activity of lyso-PC stimulated PKCζ, respectively). These results were not due to denaturation of PKCζ, because the enzyme maintains its ability to be activated by lyso-PC even after exposure to 1% Triton X-100. Finally, we considered the possibility that lyso-PC bound to PKCζ nonspecifically. To determine whether this were so, we immunoprecipitated PKCζ, Sar1b, vesicle associated membrane protein (VAMP)7, and IgG from intestinal cytosol using cytosol isolated from rats gavaged with corn oil, PC, and [^{3}H]PC. At the end of three rounds of immunodepletion, when anti-PKCζ antibody was used, 75% of the [^{3}H]PC had been removed from the cytosol but only 13% of the dpm when Sar1b was immunodepleted, 12% using anti-VAMP7 antibodies, and 9% using IgG. In sum, these data support the thesis that lyso-PC specifically binds to PKCζ and activates it.

To more directly confirm the relationship between PKCζ activation and lyso-PC concentrations in cytosol, we related PKCζ activation to lyso-PC concentration. This relationship revealed a typical saturation curve (Fig. 5C). We utilized the initial rate portion of the curve to delineate a mathematical relationship between the two variables (Fig. 5D). This would suggest that for every additional 1 nM of lyso-PC in the cytosol, PKCζ is ~20% activated.

Lyso-PC is more effective as a PKCζ activator than other phospholipids or their lyso derivatives

When lyso-PC was directly tested against PS and ceramide as an activator of PKCζ, lyso-PC was more effective than either phospholipid even though 7-fold more PS and 16-fold more ceramide than lyso-PC were used in the assay (**Fig. 6A**). Importantly, FA (oleate) was also ineffective as an activator of PKCζ. We also tested lyso-PC against the lyso derivatives of other phospholipids. Although each was an effective activator of PKCζ, lyso-PC was the most potent despite the fact that the other lyso derivatives were used at least at 20-fold greater concentrations (Fig. 6B). Because in vivo the concentrations of the lyso compounds except for lyso-PC were very low in cytosol, none of these would be expected to be effective in vivo PKCζ stimulators. Further, we found that the concentration of ceramide in cytosol did not vary under changing PC input rates into the intestine (Fig. 6C).

PKCζ elutes from CEV on activation

We next wished to see what effect exposure of PKCζ to lyso-PC had on its binding to CEV. The data presented in

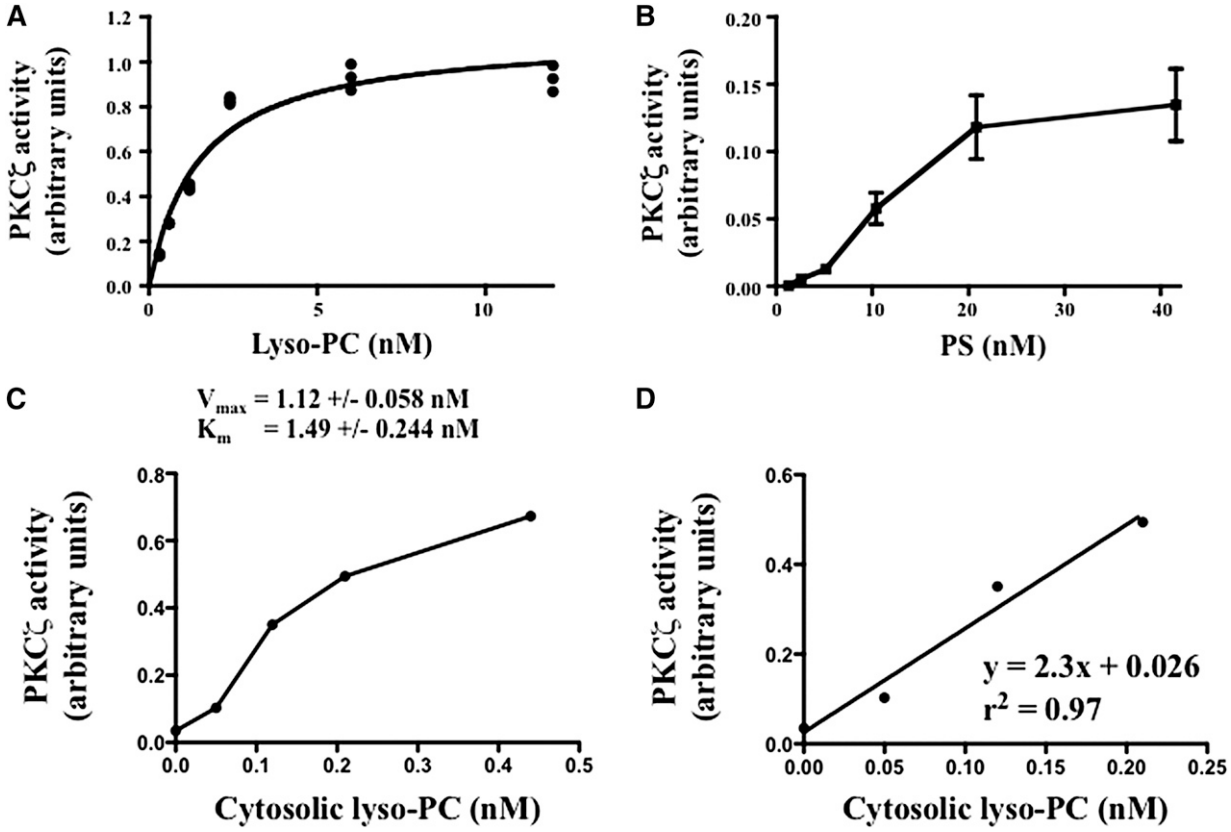

Fig. 5. PKCζ activity on the addition of varying amounts of activator and lyso-PC concentrations. PKCζ activity is expressed in arbitrary units on the ordinate after the addition of the indicated amounts of lyso-PC (A), or PS was added in the indicated amounts and PKCζ activity measured (B). rPKCζ (9 pM) was used as the enzyme source. K_m and V_{max} were calculated by the random numbers method using Prism software supplied by GraphPad Software Inc. (San Diego, CA). C: PKCζ activity as compared with varying cytosolic lyso-PC concentrations as indicated on the abscissa. PKCζ activity is expressed as arbitrary units. D: The least squares analysis of the initial rates of PKCζ activity using lyso-PC concentrations from 0 to 0.45 nM.

Fig. 7A suggest that the greater the concentration of lyso-PC in cytosol, the more PKCζ eluted from CEV. The data are consistent with the hypothesis that activation of PKCζ detaches PKCζ from CEV allowing it to diffuse in the cytosol. By contrast, other components of CEV such as caveolin-1 (Fig. 7B) and CD36 (Fig. 7C) were relatively unaffected by changes in lyso-PC concentrations and remained with the CEV. These data confirm the specificity of the effect of lyso-PC on PKCζ with respect to CEV binding.

To further confirm the effect of PKCζ activation on PKCζ binding to CEV, we tested whether PKCζ exposed to lyso-PC would bind to CEV. As shown in Fig. 7D, native CEV is replete with PKCζ (bar 1) as expected under native conditions, but on exposure to lyso-PC, CEV was nearly completely depleted of PKCζ (bar 2). Importantly, rPKCζ, activated by lyso-PC, does not repopulate CEV (bar 3). In sum, these data would suggest that activated PKCζ elutes from CEV in a vectorial fashion.

PKCζ activation is associated with a conformational change in the enzyme

The elution of PKCζ from CEV on its activation suggested the possibility that activation induces a conformational change in the kinase. To test this idea, we used limited proteolysis using trypsin on native and lyso-PC-activated rPKCζ (**Fig. 8A**). PKCζ was incubated with trypsin from 0 to 8 min as shown below the gel for both the native and activated species. Native PKCζ resisted proteolysis significantly more than activated PKCζ. Native PKCζ's silver stain signal was extinguished at 8 min of incubation as compared with 4 min for activated PKCζ. Proteolytic fragments can be seen at lower Mr than PKCζ at each time of incubation except for T = 0. Fig. 8B, C show a graphical presentation of the densitometry readings (Gel DocX) at each incubation time as a percentage of the density reading at T = 0 for nonactivated PKCζ (Fig. 8B) and activated PKCζ (Fig. 8C). The increase in the rapidity of proteolysis on activation of PKCζ is clearly evident.

CD36, caveolin-1, and PKCζ interact in vivo

Although CD36, PKCζ, and caveolin-1 were each present on CEV, we next wished to determine whether they were interactive in vivo. To test this, we performed a series of immunoprecipitation experiments (**Fig. 9**) using cytosol from PC-infused rats (see Materials and Methods). Each of the proteins studied, CD36, PKCζ, and caveolin-1, was found to immunoprecipitate the other two. When the reverse immunoprecipitations were performed, an equally strong signal was obtained confirming the specificity of the reaction.

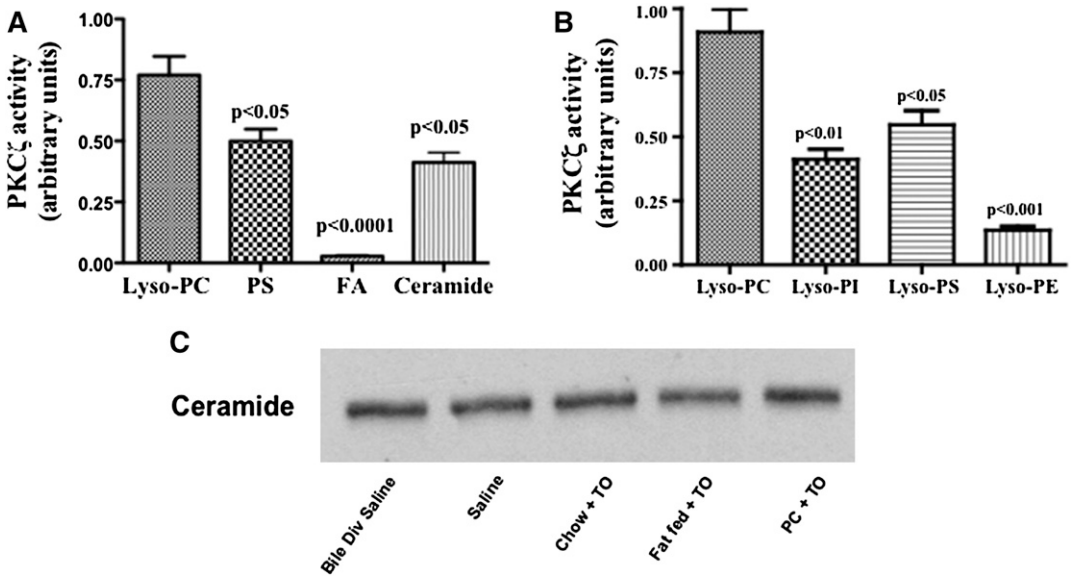

Fig. 6. PKCζ activity using varying potential activators. A: PKCζ activity using lyso-PC, PS, oleate (FA), or ceramide as activators; 6 nM, 40 nM, 1 μM, and 100 nM potential activator was added, respectively. rPKCζ (9 pM) was used as the enzyme source, and PKCζ activity was expressed as arbitrary units on the ordinate. B: PKCζ activity in response to various lyso-phospholipids as indicated on the abscissa. Lyso-PC (6 nM), lyso-PI (100 nM), lyso-PS (100 nM), and lyso-PE (100 nM) were used as activators. The data are expressed in arbitrary units on the ordinate. Significant differences between the means are indicated by *P* values above the bars. C: Immunoblot using anti-ceramide antibodies using 30 μg cytosolic protein in each lane for each model (as in Fig. 1, see Materials and Methods).

PKCζ binds to Sar1b

Finally, we wished to know whether PKCζ, once eluted from CEV, could bind to its cytosolic substrate, Sar1b. This interaction was confirmed by the co-immunoprecipitation experiments shown in Fig. 9. For these experiments, cytosol isolated from PC-infused rats (see Materials and Methods) was used to ensure that most PKCζ was eluted off CEV and was available for potential binding to Sar1b. As shown, the strongest binding to Sar1b was with PKCζ.

DISCUSSION

The present studies were undertaken to test the hypothesis that the physiological activator of PKCζ in the intestine is lyso-PC. This thesis was based on prior work that showed that chylomicron output into the lymph by the intestine was directly proportional to the amount of PC delivered to the intestine (10, 11, 13). Because the ability of the intestine to export chylomicrons presumably depends on the rate of budding of the PCTV, we thought it likely that lyso-PC, the absorbed hydrolytic product of dietary and biliary PC, would be an activator of PKCζ. This supposition was supported by our preliminary findings on ER-PCTV budding activity using bile-diverted and PC-infused rats (20), and the fact that in the absence of PKCζ, no ER-PCTV budding occurred (7, 8). Additionally, we felt that if we could correlate cytosolic lyso-PC concentrations with PCTV budding, it would more closely tie PCTV budding to chylomicron export by the intestine.

We have used primary isolates of intestinal absorptive cells for these studies. Although intestinal cell models such as the Caco2 cell and the IPEC cell have been used to study lipid absorption and transport, none of them are as efficient as intestinal cells in vivo in the transport of dietary fat. The cell models transport <10% of their TAG content, whereas rat intestine is able to turn over 60% of its TAG content per hour (13). There are a number of potential explanations for this. Caco2 cells have greatly reduced monoacylglycerol acyltransferase (MGAT) activity (21). Acylation of MAG by MGAT provides the major source of DAG substrate for TAG synthesis. TAG synthesized from MAG is more likely to be incorporated into chylomicron-TAG than if it is synthesized via the Kennedy pathway (13, 22). Further, the data reported here were obtained in intestinal epithelial cells that were exposed to lipid solely on their apical surface. Clear differences have been described in the metabolism of FAs absorbed from the basolateral membrane as compared with the apical membrane of this cell type (23). The proportion of absorbed FA utilized for TAG synthesis versus phospholipid synthesis or conversion to CO_2 is greater when the FA is presented from the apical versus the basolateral side of the membrane (24, 25). Further, studies using cell models yield differing results when performed in whole animals: apoAIV overexpression is associated with increased TAG output by IPEC cells (26, 27) but not in whole animal experiments (28). Caco2 cells also lack FABP2 that is thought to have a transport role for FA intracellularly (29). Finally, and most importantly, Caco2 cells appear to require a coat protein II mechanism for TAG to exit the ER (30, 31), whereas rat intestinal cells do not (1). In sum, these data provide a strong rationale for using whole intestine to study the molecular details of fat absorption.

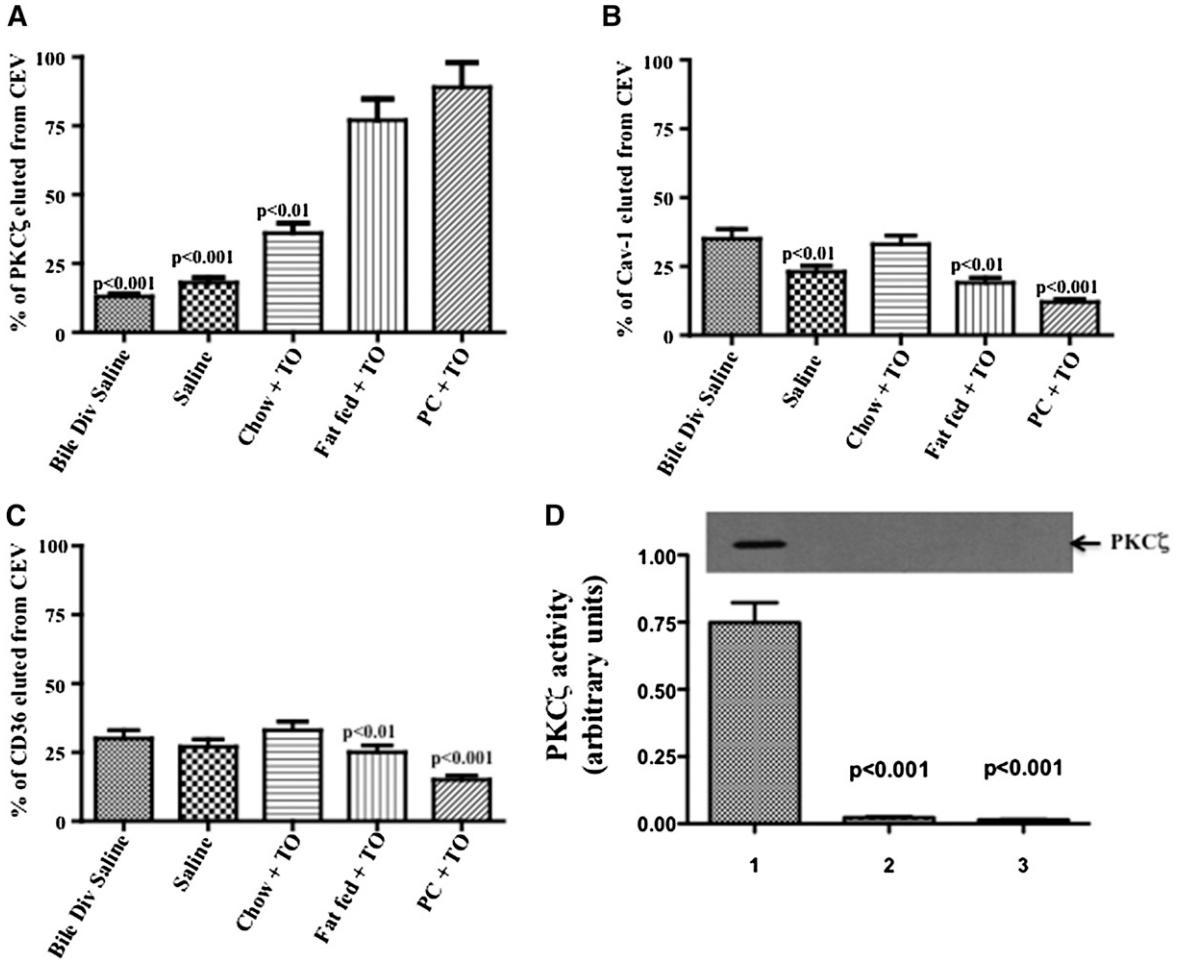

Fig. 7. The elution of PKCζ from CEV under varying physiological conditions. A: The percentage of PKCζ eluted from CEV under the same infusion conditions as in Figs. 1, 3 with caveolin-1 (B) and CD36 (C) eluted from the CEV are indicated on the ordinate. *P* values above the bars test differences between the means. D: PKCζ activity on native CEV (bar 1), CEV reisolated after PKCζ activation by lyso-PC (6 nM) (bar 2), and PKCζ activity on PKCζ-depleted CEV when incubated for 30 min with activated rPKCζ (6 nM lsyo-PC) (bar 3). *P* values test the differences between the means and are shown above the bars. The immunoblot above the bars indicates the amount of PKCζ remaining on CEV after each manipulation.

In the present study, we found that lyso-PC is a physiological activator of PKCζ. PKCζ is a member of the PKC superfamily of protein kinases, in particular it is an atypical PKC kinase. The atypical PKC's, specifically PKCζ, are stimulated by a variety of agents such as PS, arachidonic acid (32, 33), phosphatidic acid (PA), lyso-PA, phosphatidylinositol, and phosphatidylglycerol (33) but not DAG or Ca^{2+}. In intestinal cells, we show here that lyso-PC is a potent stimulator over a broad range of activator concentrations. By contrast, in prior experiments lyso-PC has been shown to be a concentration-dependent stimulator/inhibitor of PKCζ activity (32), to be a modest stimulator in a nondose ranging study (34), or to require PS for PKCζ activity to be expressed (35).

In this study, we focused on potential stimulators of PKCζ activity that could be derived from the diet. The major dietary lipids presented for absorption are FAs and MAGs derived from the lipolysis of TAG by pancreatic triacylglycerol lipase and lyso-phospholipids derived from the phospholipolysis of the phospholipids by pancreatic phospholipase A_2. The most prominent dietary phospholipid is PC, most of which comes from bile (19). The most prominent lyso-phospholipid identified in intestinal cytosol was lyso-PC, the majority of which was found in the CEV fraction using chow-fed rats. Ceramide was also considered as a potential activator because of its generation from sphingomyelin by sphingomyelinase located on the brush border of enterocytes (36, 37). Because ceramide concentrations did not vary in the cytosol over a wide range of activity changes in PKCζ and was found not to be a potent activator of PKC, it is unlikely that ceramide is a physiologically important PKCζ activator under the conditions of our experiments.

PKCζ may be activated by three different mechanisms, phosphorylation of T410 by phosphatidylinositol-3-phosphate/P DK-1, autophosphorylation of T560, and a conformational change in the kinase resulting in relief of pseudosubstrate inhibition (38). In the current experiments, ATP was required for activation, and a conformational change was observed in the kinase on activation by lyso-PC resulting in us being unable to differentiate between autophosphorylation of T560 and the presumed relief of inhibition induced by the pseudosubstrate on binding to lyso-PC.

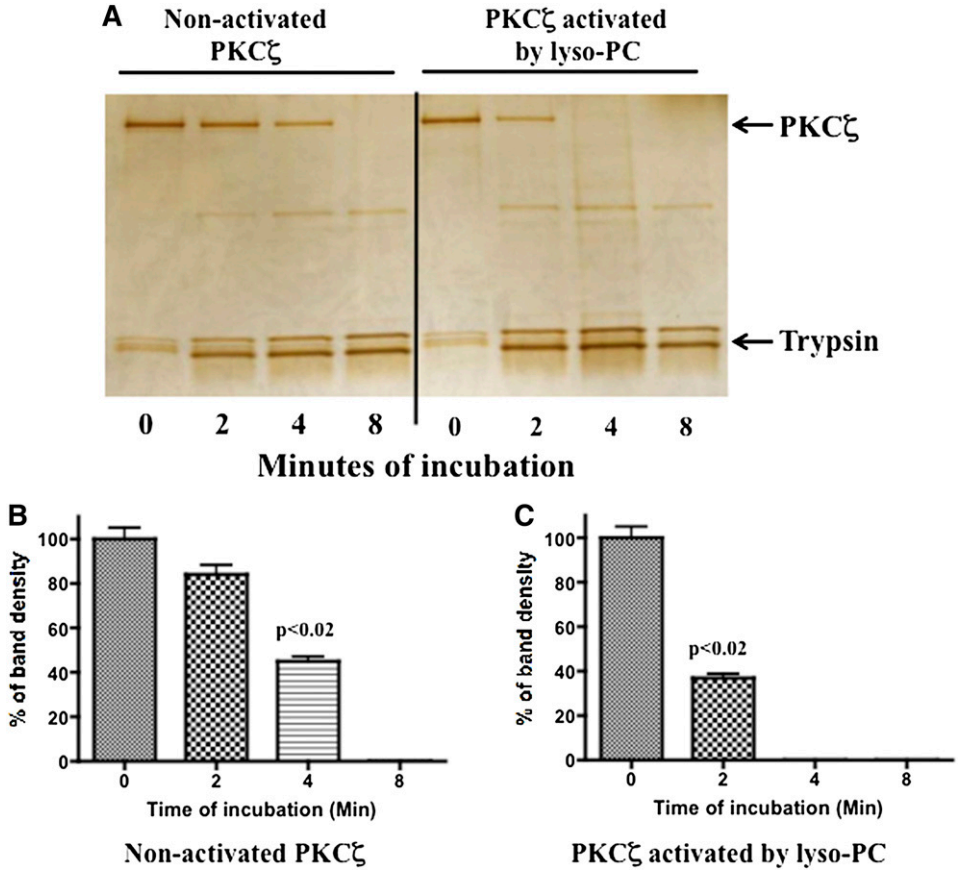

Fig. 8. Effect of limited proteolysis on PKCζ before and after activation. A: Ten micrograms of rPKCζ or rPKCζ previously activated by 6 mM lyso-PC was incubated with 5 ng trypsin at 37°C for 0 to 8 min as indicated below the lanes. Each incubation was terminated by boiling in Laemmli's buffer. The protein fragments of each sample (30 µl) were separated by SDS-PAGE and stained using the silver stain method. Whether the PKCζ was activated is indicated at the top of the gel. The minutes of tryptic incubation are shown below each lane (0–8 min). The arrows on the right-hand side of the figure show bands of PKCζ and trypsin. A line has been drawn separating nonactivated from activated PKCζ. B, C: Densitometric analysis of PKCζ at each time point after tryptic incubation expressed as a percentage of the density of staining of PKCζ at T = 0, which was 526 arbitrary units for native PKCζ (B) and 588 arbitrary units for activated PKCζ (C).

On activation, PKCζ is usually considered to move from the cytosol to a specific binding site such as tight junctions (39, 40), signaling molecules (40), or caveolae (41). By contrast, we show in the intestine that PKCζ elutes from CEV on activation. One possibility for this is that PKCζ activation most likely takes place on the surface of the CEV inducing a conformational change in PKCζ as we show here. This structural alteration results in PKCζ eluting from the surface of the CEV, enabling it to diffuse in the cytosol quicker and more easily find its substrate, Sar1b, than if it were on CEV. Once bound to Sar1b, it phosphorylates a threonine (7). The consequence of Sar1b phosphorylation is to free FABP1 from its cytosolic heterotetramer (7), enabling it to bind to the ER and organize the PCTV budding complex (4, 6, 7).

It should be noted that the major actors in the activation of PKCζ are all present on the surface of CEV. Because of this constricted geographic location, small amounts of activator could potentially have significant effects on its target as we show here with lyso-PC and PKCζ. Further, the K_m of lyso-PC activation of PKCζ and the measured concentration of lyso-PC in the cytosol in our various models would suggest that in each model, the amount of lyso-PC present would directly affect PKCζ activation.

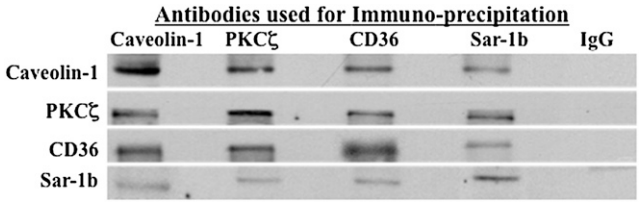

Fig. 9. Co-immunoprecipitation studies in proteins in cytosol. Bead-bound antibodies to caveolin-1, PKCζ CD36, and Sar1b were incubated with cytosol isolated from PC-infused rats (1 mg), and the beads were washed to remove unbound proteins. The beads were boiled in Laemmli's buffer, and the proteins were separated by SDS-PAGE. The proteins were transblotted to a nitrocellulose membrane, and the membrane was incubated with the indicated antibodies. Antibody binding was measured by ECL. IgG bound to beads was used as a control.

The results of our limited proteolysis experiments suggest that PKCζ bound to CEV is in a more globular form (molten globule) in which many tryptic susceptible hydrolytic sites are hidden. By contrast, on activation by lyso-PC, PKCζ presumably assumes a more open configuration resulting in more tryptic attackable sites becoming available.

Our current and past data lead us to propose a new feed forward theory of dietary fat absorption (**Fig. 10**). This theory would suggest that dietary FAs (MAG) enter the apical membrane of enterocytes via caveolae and are endocytosed as CEVs in proportion to the quantity of absorbed FAs (16). We propose that the CEVs are targeted to the ER where they unload their FA and MAG (not shown to be present in CEV) cargo. The FAs and MAG are converted to TAG in the ER, in preparation for their incorporation into prechylomicrons. On the surface of CEV is lyso-PC that has been absorbed from the lumen derived mostly from dietary (biliary) PC and PKCζ. On the surface of the CEV, lyso-PC activates PKCζ, which elutes from the vesicle, binds to, and phosphorylates Sar1b as a member of an FABP1-containing heteroquatromer in intestinal cytosol (7). As a complex member, FABP1 cannot bind to the ER (7). Sar1b phosphorylation disrupts the complex, releasing FABP1, which can now bind to the ER membrane. On binding, FABP1 organizes the PCTV budding complex generating the vesicle that transports the prechylomicron to the Golgi (4, 6). The result of the proposed mechanism is that the ability of the ER to generate and transport prechylomicrons is controlled, at least in part, by the amount of dietary FA delivered to the ER as substrate for chylomicron TAG. This is consistent with the more FAs absorbed, the more CEVs are produced (16). This would provide a potential mechanism whereby the amount of dietary FA could correlate with PCTV production. Although luminal PC availability also controls chylomicron and PCTV output (9, 11, 13, 20, 42), it should be recognized that the more lipid ingested, the greater the gall bladder contraction and thus PC delivery to the intestine. Thus, the amount of dietary lipid and PC delivery to the intestine is mutually supportive.

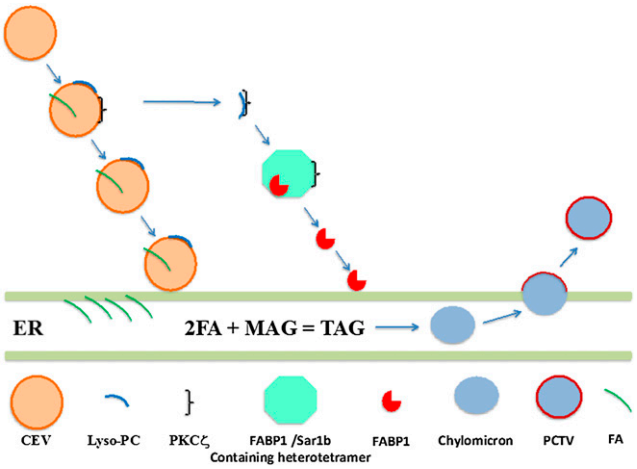

Fig. 10. Schema of the self-regulation of dietary fat absorption. Dietary fat enters the enterocyte as FA or MAG and is endocytosed into the cytoplasm via CEV in proportion to the dietary intake. On the surface of the CEV is PKCζ and lyso-PC. The lyso-PC activates PKCζ that elutes off the CEV and diffuses into the cytosol. FA (MAG)-containing CEV targeted to the ER where it unloads its FA cargo. The FA and MAG are used as substrates for TAG synthesis, which is incorporated into the prechylomicron. Simultaneously, the activated PKCζ binds to and phosphorylates Sar1b, which disrupts the Sar1b-FABP1-containing heterodimer. The FABP1 is targeted to the ER where it organizes the PCTV budding complex.

REFERENCES

1. Siddiqi, S. A., F. S. Gorelick, J. T. Mahan, and C. M. Mansbach II. 2003. COPII proteins are required for Golgi fusion but not for endoplasmic reticulum budding of the pre-chylomicron transport vesicle. *J. Cell Sci.* **116:** 415–427.
2. Mansbach, C. M., and R. Dowell. 2000. Effect of increasing lipid loads on the ability of the endoplasmic reticulum to transport lipid to the Golgi. *J. Lipid Res.* **41:** 605–612.
3. Mansbach II, C. M., and P. Nevin. 1998. Intracellular movement of triacylglycerols in the intestine. *J. Lipid Res.* **39:** 963–968.
4. Siddiqi, S., U. Saleem, N. A. Abumrad, N. O. Davidson, J. Storch, S. A. Siddiqi, and C. M. Mansbach II. 2010. A novel multiprotein complex is required to generate the prechylomicron transport vesicle from intestinal ER. *J. Lipid Res.* **51:** 1918–1928.
5. Siddiqi, S., S. A. Siddiqi, and C. M. Mansbach II. 2010. Sec24C is required for docking the prechylomicron transport vesicle with the Golgi. *J. Lipid Res.* **51:** 1093–1100.
6. Neeli, I., S. A. Siddiqi, S. Siddiqi, J. Mahan, W. S. Lagakos, B. Binas, T. Gheyi, J. Storch, and C. M. Mansbach II. 2007. Liver fatty acid-binding protein initiates budding of pre-chylomicron transport vesicles from intestinal endoplasmic reticulum. *J. Biol. Chem.* **282:** 17974–17984.
7. Siddiqi, S., and C. M. Mansbach II. 2012. Phosphorylation of Sar1b protein releases liver fatty acid-binding protein from multiprotein complex in intestinal cytosol enabling it to bind to endoplasmic reticulum (ER) and bud the pre-chylomicron transport vesicle. *J. Biol. Chem.* **287:** 10178–10188.
8. Siddiqi, S. A., and C. M. Mansbach II. 2008. PKC zeta-mediated phosphorylation controls budding of the pre-chylomicron transport vesicle. *J. Cell Sci.* **121:** 2327–2338.
9. Tso, P., M. Kendrick, J. A. Balint, and W. J. Simmonds. 1981. Role of biliary phosphatidylcholine in the absorption and transport of dietary triolein in the rat. *Gastroenterology.* **80:** 60–65.
10. Tso, P., J. A. Balint, and W. J. Simmonds. 1977. Role of biliary lecithin in lymphatic transport of fat. *Gastroenterology.* **73:** 1362–1367.
11. Voshol, P. J., D. M. Minich, R. Hayinga, R. P. Elferink, H. J. Verkade, A. K. Groen, and F. Kuipers. 2000. Postprandial chylomicron formation and fat absorption in multidrug resistance gene 2 P-glycoprotein-deficient mice. *Gastroenterology.* **118:** 173–182.
12. Knox, R., I. Stein, D. Levinson, P. Tso, and C. M. Mansbach II. 1991. Effect of fat pre-feeding on bile flow and composition in the rat. *Biochim. Biophys. Acta.* **1083:** 65–70.
13. Mansbach II, C. M., and A. Arnold. 1986. Steady-state kinetic analysis of triacylglycerol delivery into mesenteric lymph. *Am. J. Physiol.* **251:** G263–G269.
14. Nevin, P., D. Koelsch, and C. M. Mansbach II. 1995. Intestinal triacylglycerol storage pool size changes under differing physiological conditions. *J. Lipid Res.* **36:** 2405–2412.
15. Weiser, M. M. 1973. Intestinal epithelial cell surface membrane glycoprotein synthesis: I. An indicator of cellular differentiation. *J. Biol. Chem.* **248:** 2536–2541.
16. Siddiqi, S., A. Sheth, F. Patel, M. Barnes, and C. M. Mansbach II. 2013. Intestinal caveolin-1 is important for dietary fatty acid absorption. *Biochim. Biophys. Acta.* **1831:** 1311–1321.
17. McHowat, J., and P. B. Corr. 1993. Thrombin-induced release of lysophosphatidylcholine from endothelial cells. *J. Biol. Chem.* **268:** 15605–15610.

18. Wientzek, M., G. Arthur, R. Y. Man, and P. C. Choy. 1985. A sensitive method for the quantitation of lysophosphatidylcholine in canine heart. *J. Lipid Res.* **26:** 1166–1169.
19. Borgström, B. 1976. Phospholipid absorption. *In* Lipid Absorption: Biochemical and Clinical Aspects. K. Rommel and H. Goebel, editors. MTP Press, Lancaster, England. 65–72.
20. Kumar, N. S., and C. M. Mansbach. 1997. Determinants of triacylglycerol transport from the endoplasmic reticulum to the Golgi in intestine. *Am. J. Physiol.* **273:** G18–G30.
21. Trotter, P. J., and J. Storch. 1993. Fatty acid esterification during differentiation of the human intestinal cell line CaCo-2. *J. Biol. Chem.* **268:** 10017–10023.
22. Mansbach II, C. M., and R. F. Dowell. 1992. Uptake and metabolism of circulating fatty acids by rat intestine. *Am. J. Physiol.* **263:** G927–G933.
23. Trotter, P. J., and J. Storch. 1991. Fatty acid uptake and metabolism in a human intestinal cell line (Caco-2): comparison of apical and basolateral incubation. *J. Lipid Res.* **32:** 293–304.
24. Gangl, A., and R. K. Ockner. 1975. Intestinal metabolism of plasma free fatty acids: intracellular compartmentation and mechanisms of control. *J. Clin. Invest.* **55:** 803–813.
25. Gangl, A., and F. Renner. 1978. In vivo metabolism of plasma free fatty acids by intestinal mucosa of man. *Gastroenterology.* **74:** 847–850.
26. Lu, S., Y. Yao, X. Cheng, S. Mitchell, S. Leng, S. Meng, J. W. Gallagher, G. S. Shelness, G. S. Morris, J. Mahan, et al. 2006. Overexpression of apolipoprotein A-IV enhances lipid secretion in IPEC-1 cells by increasing chylomicron size. *J. Biol. Chem.* **281:** 3473–3483.
27. Lu, S., Y. Yao, S. Meng, X. Cheng, and D. D. Black. 2002. Overexpression of apolipoprotein A-IV enhances lipid transport in newborn swine intestinal epithelial cells. *J. Biol. Chem.* **277:** 31929–31937.
28. Kohan, A. B., F. Wang, X. Li, A. E. Vandersall, S. Huesman, M. Xu, Q. Yang, D. Lou, and P. Tso. 2013. Is apolipoprotein A-IV rate limiting in the intestinal transport and absorption of triglyceride? *Am. J. Physiol. Gastrointest. Liver Physiol.* **304:** G1128–G1135.
29. Gedde-Dahl, A., M. A. Kulseth, T. Ranheim, C. A. Drevon, and A. C. Rustan. 2002. Reduced secretion of triacylglycerol in CaCo-2 cells transfected with intestinal fatty acid-binding protein. *Lipids.* **37:** 61–68.
30. Jones, B., E. L. Jones, S. A. Bonney, H. N. Patel, A. R. Mensenkamp, S. Eichenbaum-Voline, M. Rudling, U. Myrdal, G. Annesi, N. Sandhia, et al. 2003. Mutations in a Sar1 GTPase of COPII vesicles are associated with lipid absorption disorders. *Nat. Genet.* **34:** 29–31.
31. Levy, E., E. Harmel, M. Laville, R. Sanchez, L. Emonnot, D. Sinnett, E. Ziv, E. Delvin, P. Couture, V. Marcil, et al. 2011. Expression of Sar1b enhances chylomicron assembly and key components of the coat protein complex II system driving vesicle budding. *Arterioscler. Thromb. Vasc. Biol.* **31:** 2692–2699.
32. Müller, G., M. Ayoub, P. Storz, J. Rennecke, D. Fabbro, and K. Pfizenmair. 1995. PKCz is a molecular switch in signal transduction of TNF-a, bifunctionally regulated by ceramide and arachidonic acid. *EMBO J.* **14:** 1961–1969.
33. Limatola, C., D. Schaap, W. H. Moolenaar, and W. J. van Blitterswijk. 1994. Phosphatidic acid activation of protein kinase C-zeta overexpressed in COS cells: comparison with other protein kinase C isotypes and other acidic lipids. *Biochem. J.* **304:** 1001–1008.
34. Scott, G. A., M. Arioka, and S. E. Jacobs. 2007. Lysophosphatidylcholine mediates melanocyte dendricity through PKCzeta activation. *J. Invest. Dermatol.* **127:** 668–675.
35. Kugiyama, K., M. Ohgushi, S. Sugiyama, T. Murohara, K. Fukunaga, E. Miyamoto, and H. Yasue. 1992. Lysophosphatidylcholine inhibits surface receptor-mediated intracellular signals in endothelial cells by a pathway involving protein kinase C activation. *Circ. Res.* **71:** 1422–1428.
36. Zhang, J. H., L. Ge, W. Qi, L. Zhang, H. H. Miao, B. L. Li, M. Yang, and B. L. Song. 2011. The N-terminal domain of NPC1L1 protein binds cholesterol and plays essential roles in cholesterol uptake. *J. Biol. Chem.* **286:** 25088–25097.
37. Duan, R. D., L. Nyberg, and A. Nilsson. 1995. Alkaline sphingomyelinase activity in rat gastrointestinal tract: distribution and characteristics. *Biochim. Biophys. Acta.* **1259:** 49–55.
38. Standaert, M. L., G. Bandyopadhyay, Y. Kanoh, M. P. Sajan, and R. V. Farese. 2001. Insulin and PIP3 activate PKC-zeta by mechanisms that are both dependent and independent of phosphorylation of activation loop (T410) and autophosphorylation (T560) sites. *Biochemistry.* **40:** 249–255.
39. Whyte, J., L. Thornton, S. McNally, S. McCarthy, F. Lanigan, W. M. Gallagher, T. Stein, and F. Martin. 2010. PKCzeta regulates cell polarisation and proliferation restriction during mammary acinus formation. *J. Cell Sci.* **123:** 3316–3328.
40. Hirai, T., and K. Chida. 2003. Protein kinase Czeta (PKCzeta): activation mechanisms and cellular functions. *J. Biochem.* **133:** 1–7.
41. Yang, Z., W. Sun, and K. Hu. 2009. Adenosine A(1) receptors selectively target protein kinase C isoforms to the caveolin-rich plasma membrane in cardiac myocytes. *Biochim. Biophys. Acta.* **1793:** 1868–1875.
42. Tso, P., J. Lam, and W. J. Simmonds. 1978. The importance of the lysophosphatidylcholine in lymphatic transport of fat. *Biochim. Biophys. Acta.* **528:** 364–372.